Analyzing the Impedance Resonance of Piezoelectric Stacks

S. Sherrit, S.P. Leary, Y. Bar-Cohen and B.P. Dolgin
Jet Propulsions Laboratory, Mail Stop 82-105, 4800 Oak Grove Blvd, Pasadena, CA, 91109-8099
R. Tasker
TASI Technical Software Inc., 444 Frontenac St., Kingston, Ontario, K7L 3T4, Canada

Abstract – Inversion techniques to determine the complex material constants from the impedance data of a zero bond-length stack resonator are studied. The impedance equation examined in this paper is based on the derivation by Martin [G.E. Martin, JASA, 36, pp. 1496-1506, 1964]. The asymptotic solutions for the case where the number of layers n is large (n>8) and n small (n≤2) are presented in terms of the complex material constants of the piezoelectric. When n = 1 or 2, it is shown that the wave speed in the stack is determined by the open circuit elastic constant s^D_{33}. In the limit of large n, the wave speed is determined by the short circuit elastic constant s^E_{33}. Techniques to invert the impedance data to determine complex material constants are presented for all values of n. The error associated with using the impedance equations derived from fully short and fully open electrical boundary conditions is investigated. Since the model is based on material properties rather than circuit constants, it allows for the direct evaluation of specific ageing or degradation mechanisms.

I. INTRODUCTION

Piezoelectric stacks are used in a variety of applications that require relatively high stress and larger strain than single element piezoelectric transducers can produce. These include micro-positioning systems, solid-state pumps/switches, noise isolation mounts, ultrasonic drills and stacked ultrasonic transducers. The solution for the zero bond length stack was derived by Martin [1], [2]. His model was derived from Mason's equivalent circuit of n layers connected mechanically in series and electrically in parallel as shown in Figure 1.

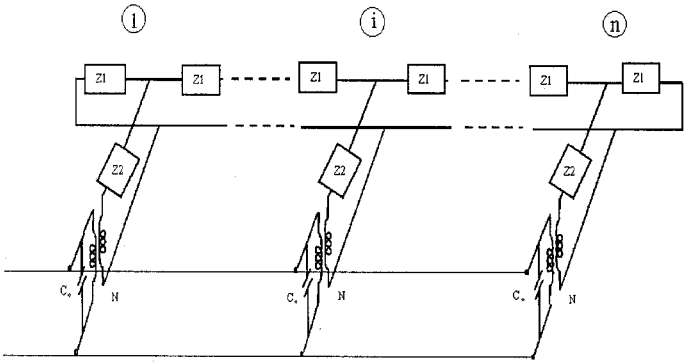

Figure 1. Equivalent circuit representation of a stack with the mechanical ports of each equivalent circuit representing a layer connected in series and n electrical ports in parallel.

II. THEORY

Martin's general solution for the admittance of a piezoelectric stack of area A, n layers and total length nL is

$$Y(\omega) = i\omega n C_0 + \frac{2N^2}{Z_{ST}} \tanh\left(\frac{n\gamma}{2}\right) \tag{1}$$

where

$$C_0 = \frac{\varepsilon_{33}^T A}{L}(1-k_{33}^2) \tag{2}$$

$$N = \frac{A}{L}\frac{d_{33}}{s_{33}^E} \tag{3}$$

$$Z_{ST} = \left(Z_1 Z_2\left(2+\frac{Z_1}{Z_2}\right)\right)^{1/2} \tag{4}$$

$$\gamma = 2\,\mathrm{arcsin}\,h\left(\left(\frac{Z_1}{2Z_2}\right)^{1/2}\right) \tag{5}$$

$$Z_1 = i\rho v^D A \tan\left(\frac{\omega L}{2v^D}\right) \tag{6}$$

$$Z_2 = \frac{\rho v^D A}{i\sin\left(\frac{\omega L}{v^D}\right)} + \frac{iN^2}{\omega C_0} \tag{7}$$

and $v^D = 1/\sqrt{\rho s_{33}^D}$ is the acoustic velocity at constant electric displacement. The constants ε_{33}^T, s_{33}^D, d_{33} are the free permittivity, the elastic compliance at constant electric displacement and the piezoelectric charge coefficient, respectively. Using equations 1 to 7, Martin demonstrated that in the limit of large n (n>8), the acoustic wave speed in the material was determined by the constant field elastic constant s_{33}^E ($v^E = 1/\sqrt{\rho s_{33}^E}$). In the limit of n > 8 an analytical equation for the admittance was presented which allowed for direct determination of material constants from the admittance data [3]. In this limit the admittance was shown to be:

$$\mathbf{Y} = \frac{iAn\omega\varepsilon_{33}^T}{L}\left(1-(\mathbf{k}_{33})^2 + \frac{(\mathbf{k}_{33})^2}{\frac{\omega}{4f_S}}\tan\left(\frac{\omega}{4f_S}\right)\right) \tag{8}$$

where the series resonance frequency is:

$$f_S = \frac{1}{2nL}\sqrt{\frac{1}{\rho \mathbf{s}_{33}^E}} \tag{9}$$

In addition to the many layer approximation discussed by Martin, equations 1 to 7 can be shown to reduce to another exact analytical solution in the limit of n = 1 or 2:

$$\mathbf{Z}= \frac{L}{\left[i\omega n\varepsilon_{33}^{T}\left(1-\mathbf{k}_{33}^{2}\right)A\right]}\left[1-\frac{\mathbf{k}_{33}^{2}\tan(\omega/4f_p)}{(\omega/4f_p)}\right] \qquad (10)$$

The wave propagates at a speed $v^D = 1/\sqrt{\rho s_{33}^D}$ that is a function of the elastic compliance at constant electric displacement. The parallel frequency constant is:

$$f_P = \frac{1}{2nL}\sqrt{\frac{1}{\rho \mathbf{s}_{33}^D}}. \qquad (11)$$

Equations 8 and 10 can be use to analyze data for stacks with many layers (n>8) and stacks with n = 1 or 2 using Smits' method [4] to determine the effective complex material properties of the piezoelectric material.

An alternative approach is to directly fit equation 1 to the data using non-linear regression techniques for complex parameters as has been done for bulk [5] and thin film [6] resonators. A modified Levenberg-Marquardt (LM) regression routine for Martin's stack solution was developed. The LM routine used a hybrid algorithm of steepest descent and inverse Hessian matrix methods to minimize χ^2 during each iteration of the algorithm. We defined the χ^2 for this system as

$$\chi^2 = \sum_i^n \left(\frac{\Delta G_i^2}{\sigma_{Gi}^2} + \frac{\Delta B_i^2}{\sigma_{Bi}^2} + \frac{\Delta R_i^2}{\sigma_{Ri}^2} + \frac{\Delta X_i^2}{\sigma_{Xi}^2} \right) \qquad (12)$$

where the Δ's are the difference terms between the data and the model at each point i. The χ^2 shown above uses both admittance and impedance data to determine the best fit. The sigma values are weighting terms for each point in the spectra.

III. RESULTS

In order to look at the transition between constant D and constant E acoustic wave speeds, the impedance/admittance was calculated as a function of frequency for n = 1 to 10 using equations 1 to 7 and the material properties shown in Table 1. The conductance determined from this calculation is shown in Figure 2. The total stack length was kept fixed. In the case n = 1, 2, the first and second series resonance frequencies are independent of n. For n>3, a shift in the second series resonance frequency is seen, caused by transition from constant D to constant E elastic boundary conditions.

To determine the magnitude of error in material constants determined from limiting equations 8 and 10, impedance data was analyzed using Smits method as a function of the number of layers. The coupling and elastic stiffness at constant electric displacement are shown in Figures 3 and 4. In the limit of large n, the real and imaginary part of the coupling coefficient determined using equation 8 approaches the input value. For n = 1, 2, the results determined using equation 10 are exact and error increases asymptotically to differences of 2.7% in the real and 6.7% in the imaginary part of the coupling coefficient. Similar deviations from the input values are seen for the analysis using equation 8 when n = 1, 2.

Table 1: The effective material properties for the data of the stack resonator shown in Figure 2. The stack length nL = 0.02m, Area A = $(0.01)^2$ m^2 and density ρ = 7800 kg/m^3.

Property	Real	Imaginary
s_{33}^E (m^2/N)	2.00×10^{-11}	-3.00×10^{-13}
ε_{33}^T (F/m)	3.085×10^{-8}	-6.17×10^{-10}
d_{33} (C/N)	3.925×10^{-10}	-7.66×10^{-12}
k_{33}	0.50	-0.001

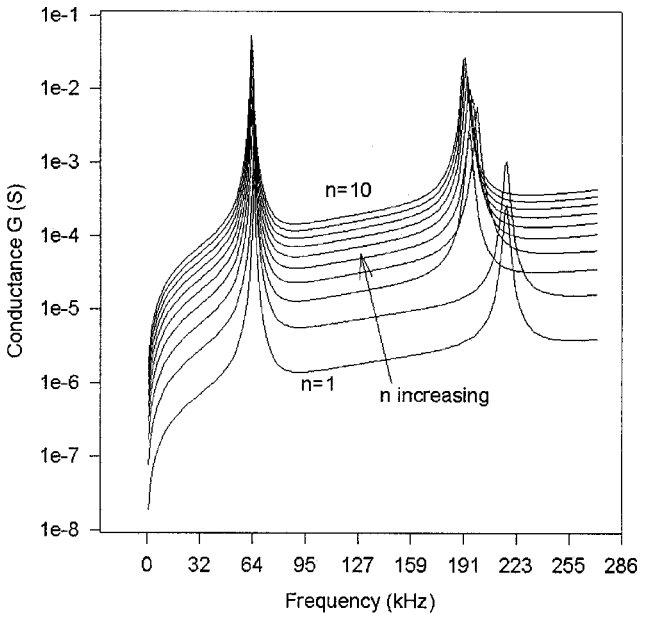

Figure 2. The conductance as a function of frequency for n=1 to 10 layers.

Figure 4 shows similar behavior for the elastic compliance determine by Smits' method using the two limiting equations. At n=1, 2, the analyzed results are equal to the input value for the impedance equation determined from the assumption of constant D boundary conditions (eqn. 10). As n increases the elastic stiffness determined from the fit to the constant E equation (eqn. 8) approaches the input value. Comparable behavior is seen in the imaginary component (loss $Q=Re(s^E)/Im(s^E)$).

It is apparent from the previous discussion that in the limit of n=1,2 or n>8 that the equations 8 and 10 can

be used to determine material properties to sufficient accuracy. For n = 3 to n = 8, errors on the order of 3% for

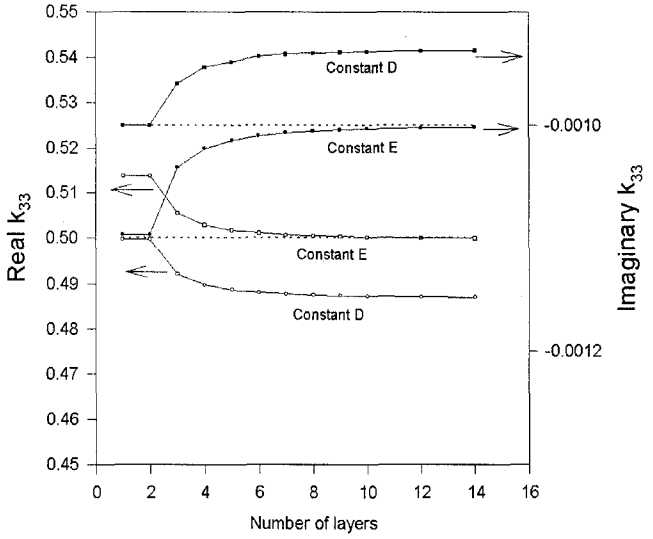

Figure 3. The electromechanical coupling constant k_{33} determined using Smits' method with the impedance equations determined from constant D and constant E elastic boundary conditions. Doted lines are the real (bottom) and imaginary (top) parts of the input k_{33}.

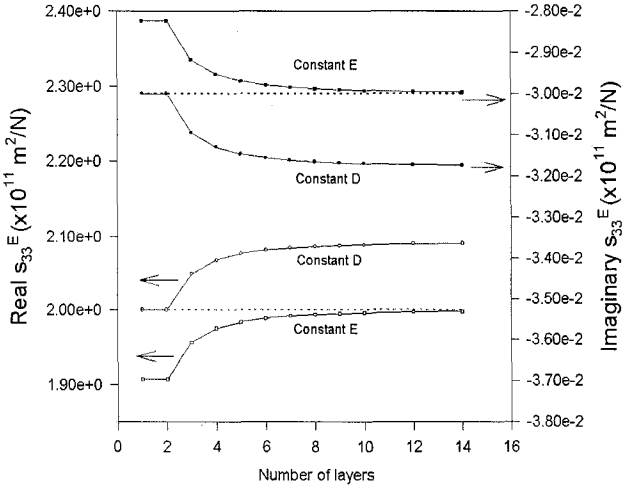

Figure 4. The elastic compliance s_{33}^E determined using Smits' method with the impedance equations determined from constant D and constant E elastic boundary conditions. Doted lines are the real (bottom) and imaginary (top) parts of the input s_{33}^E.

the coupling constant and 6% for the elastic constant are found. These errors were found to increase to 6% and 20% for a coupling of $k_{33} = 0.75$.

To evaluate the LM non-linear regression routine, impedance data generated from equation 1 and Table 1 were used along with starting values determined using Smits' method with equations 8 and 10. In all cases, the results of non-linear regression were found to converge to the input data within numerical limits and exact fits to generated spectra were found. In order to simulate real data, random noise was added to the n = 3 spectrum by multiplying R and X by (1+ xr) where x was a fractional percent and r was a random number between 1 and -1. The n = 3 spectrum resulted in the largest error in parameters from either of the asymptotic solutions. The spectrum and its fit are shown in Figure 5 for x = 0.1 (10% error). The fit was found to overlap the data. The results of the analysis for this spectrum are shown in Table 2.

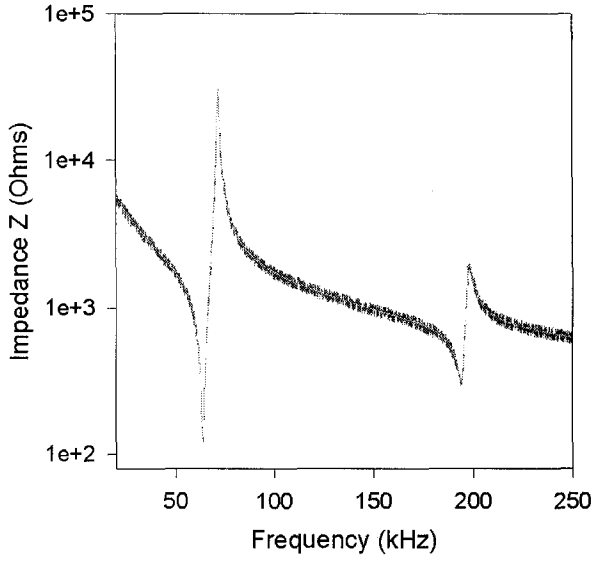

Figure 5. The impedance spectra (n=3) with random error (10%) added and the fit to the spectra using the modified Levenberg Marquardt non-linear regression routine. The data and the fit are seen to overlap. A similar fit is found in the phase versus frequency plot.

Table 2: The effective material properties for the data for the stack resonator shown in Figure 5. The stack length nL = 0.02m, Area A = $(0.01)^2$ m^2 and density ρ = 7800 kg/m^3.

Property	Real	Imaginary
s_{33}^E (m^2/N)	$2.00x10^{-11}$	$-2.98x10^{-13}$
ε_{33}^T (F/m)	$3.071x10^{-8}$	$-5.55x10^{-10}$
d_{33} (C/N)	$3.915x10^{-10}$	$-7.16x10^{-12}$
k_{33}	0.499	-0.00089

The error in the real part of the material coefficients is less than 1 % while the error in the loss components with the exception of the elastic constant is of the order of 10%.

The impedance spectra for well-aged Morgan Matroc stacks (PZT 4S) were measured using a Solartron 1260 impedance analyzer. Impedance spectra of the stack leads were taken to determine the short circuit corrections for the holder and leads. The overall dimensions of the stack were measured using a micrometer. The number of

layers was determined with an optical microscope. The effective density was determined by removing the leads of one of the stacks, and measuring the mass of the stack, and dividing by the stack volume. The stack impedance resonance spectrum is shown in Figure 6 for one of the Morgan Matroc stacks. The first major resonance is the length extensional resonance of the stack. The smaller resonances above f_p are due to resonance in the lateral direction. The spectra were fit using the non-linear regression analysis and the results are shown in Figure 6. The fit to both the impedance and phase is shown. It should be noted that these stack samples differ from an ideal stack in that they have a small aspect ratio (1:1), contain end-caps (0.6mm PZT), and the internal electrodes are discontinuous and do not cover the full cross sectional area of the stack.

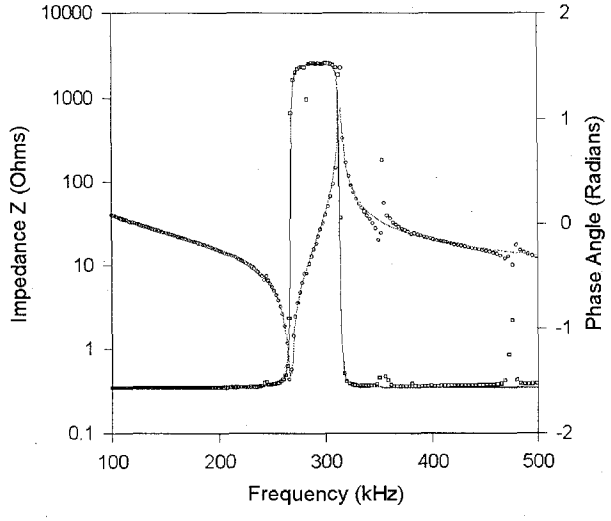

Figure 6. The impedance spectra of a Morgan Matroc stack and the fit (lines) to the spectra (symbols) using the modified Levenberg Marquardt non-linear regression routine. The data and the model are seen to overlap.

Table 3: The material properties for the Morgan Matroc stack resonator shown in Figure 6. The stack length nL = 0.00501m, effective area A = $1.9\text{x}10^{-5}$ m^2 density ρ = 7794 kg/m^3, and n = 28. The data was found to agree with the manufacturers specifications.

Property	Real	Imaginary
s_{33}^E (m^2/N)	$1.80\text{x}10^{-11}$	$-8.8\text{x}10^{-14}$
ε_{33}^T (F/m)	$1.27\text{x}10^{-8}$	$-4.0\text{x}10^{-11}$
d_{33} (C/N)	$2.80\text{x}10^{-10}$	$-1.8\text{x}10^{-12}$
k_{33}	0.587	-0.0014

Impedance measurements are usually a small signal excitation. In the majority of applications where a stack is used, the sample is driven at high fields and low frequencies. The degree to which the small signal measurement agrees with data from quasi-static high field measurements depends primarily on whether the material is hard (high coercive field) or soft (low coercive field) [7]. For a material that is soft, the dielectric and piezoelectric constant are found to depend linearly on the size of the drive field up to the coercive field where domains begin to switch [8]. For example, in the Motorola 3203HD material both the piezoelectric and dielectric constants were found to double their small signal values at fields approaching the coercive field of the material. For harder materials the field dependence is less pronounced.

Another possible limitation of small signal measurements is the frequency of measurement. For quasi-static devices that operate at low frequency, the permittivity and piezoelectric constant are slightly higher due to an intrinsic dispersion in material properties. It is apparent that small signal resonance measurements are in effect a baseline measurement, which allows for the investigation of stack material parameters in the linear reversible regime under isothermal conditions.

IV. Conclusions

A model for the impedance resonance of a stack resonator was studied which allowed for non-destructive evaluation of the material properties of the stack. A set of multi-layer stack resonators were tested and the impedance spectra fit using various models. The constants determined from fitting the data were found to be in good agreement with manufacturers specifications.

V. References

[1]G.E. Martin, "Vibrations of Coaxially Segmented Longitudinally Polarized Ferroelectric Tubes", JASA **36**, pp. 1496-1506, August 1964.

[2]G.E. Martin, "On the Theory of Segmented Electromechanical Systems" JASA, **36**, pp 1366-1370.

[3]G.E. Martin,"New Standard for Measurements of Certain Piezoelectric Ceramics" JASA, **35**, pp.925(L), 1963

[4] J.G. Smits, "Iterative Method for Accurate Determination of the Real and Imaginary Parts of Materials Coefficients of Piezoelectric Ceramics, IEEE Trans on Sonics and Ultrasonics, (SU-23),(6), pp. 393-402, November, 1976.

[5] K.W. Kwok, H.L. Chan, C.L. Choy, " Evaluation of the Material Parameters of Piezoelectric Materials by Various Methods", IEEE Trans. on Ultrasonics, Ferroelectrics and Frequency Control, **44**, (4), pp. 733-742, July 1997

[6]M. Lukacs, T. Olding, M. Sayer, R. Tasker, and S. Sherrit, " Thickness mode material constants of a supported piezoelectric film" , J. Appl. Phys. **85**, pp. 2835-2843, March 1999

[7]BERLINCOURT, H.H.A. Krueger, "Domain Processes in Lead Titanate Zirconate and Barium Titanate Ceramics", J. Appl. Phys., **30**, (11), pp. 1804-1810, 1959.

[8] S. Sherrit, H.D. Wiederick, B.K. Mukherjee, M. Sayer "Field dependence of the complex piezoelectric, dielectric, and elastic constants of Motorola PZT 3203 HD ceramic", Proc. SPIE Vol.

3040, p. 99-109, Smart Structures and Materials 1997: Smart Materials Technologies, Wilbur C. Simmons; Ilhan A. Aksay; Dryver R. Huston; Eds.